Instance-Conditional Knowledge Distillation for Object Detection

Zijian Kang[*]
Xi'an Jiaotong University
kzj123@stu.xjtu.edu.cn

Peizhen Zhang[*]
MEGVII Technology
zhangpeizhen@megvii.com

Xiangyu Zhang
MEGVII Technology
zhangxiangyu@megvii.com

Jian Sun
MEGVII Technology
sunjian@megvii.com

Nanning Zheng
Xi'an Jiaotong University
nnzheng@mail.xjtu.edu.cn

Abstract

Despite the success of Knowledge Distillation (KD) on image classification, it is still challenging to apply KD on object detection due to the difficulty in locating knowledge. In this paper, we propose an instance-conditional distillation framework to find desired knowledge. To locate knowledge of each instance, we use observed instances as condition information and retrieve knowledge by a learnable conditional decoding module. Specifically, information of each instance that a specifies condition is encoded as query and teacher's information is presented as key. We use the attention between query and key to measure the correlation, formulated by the transformer decoder. Lastly, we perform distillation on retrieved knowledge and introduce a localization-recognition-sensitive auxiliary task to optimize the decoding module. Extensive experiments demonstrate the efficacy of our method: we observe impressive improvements under various settings. Notably, we boost RetinaNet with ResNet-50 backbone from 37.4 to 40.7 mAP ($+3.3$) under $1\times$ schedule, that even surpasses the teacher (40.4 mAP) with ResNet-101 backbone under $3\times$ schedule.

1 Introduction

Deep learning applications blossom with the breakthrough of Deep Neural Networks (DNNs) [17, 24, 21] in recent years. In pursuit of high performance, advanced DNNs usually stack tons of blocks with millions of parameters, which are computation and memory consuming. The heavy design hinders the deployment of many practical downstream applications like object detection in resource-limited devices. Plenty of techniques have been proposed to address this issue, like network pruning [15, 27, 18], quantization [22, 23, 35], mobile architecture design [38, 39] and knowledge distillation [19, 37, 43] (KD). Among them, KD is one of the most popular choices, since it can boost a target network without introducing extra inference-time burden or modifications.

KD is popularized by Hinton *et al.* [19], where knowledge from a strong pretrained teacher network is transferred to a small target student network. Many good works emerge to further improve the classification results following Hinton [50, 37, 32]. However, these methods for image classification are sub-optimal in the detection scenario and obtain only slight improvement [28, 51]. We attribute the reason to two differences: (1) Other than category classification, another challenging goal to localize the object is hardly taken into the consideration. (2) Multiple target objects are presented in

[*] Equal contribution.

35th Conference on Neural Information Processing Systems (NeurIPS 2021).

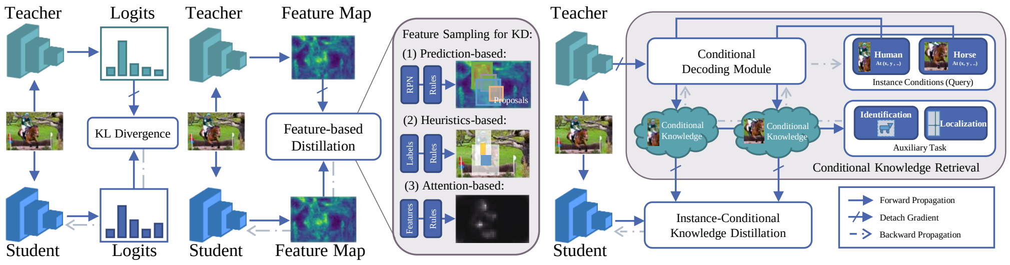

(a) KD [19]. (b) Conventional detection KD. (c) Ours: Instance-conditional KD.

Figure 1: Compare with different methods for knowledge distillation. (a) KD [19] for classification transfers logits. (b) Recent methods for detection KD distill intermediate features, different region-based sampling methods are proposed. (c) Our method explicitly distill the desired knowledge.

an image for detection, which makes features of objects distribute in different locations. Due to these reasons, the knowledge becomes rather ambiguous in detection, which makes distillation challenging.

To implement KD for detection, previous methods normally distill the intermediate feature representations to cover the whole picture. The challenge above is therefore usually addressed as where to transfer between student and teacher detector. Existent works could be divided into three types according to the feature sampling paradigm: prediction-based, heuristic-based and attention-based. In prediction-based methods [28, 11, 6], proposal regions predicted by the RPN [36] or detector are sampled for distillation. In heuristics-based methods [14, 45], manually selected regions like foreground or label-assigned regions are sampled. Despite the success of these methods, limitations still exist, e.g., many methods neglect the informative context regions or involve meticulous decisions. Recently, Zhang *et al.* [51] propose the attention-based method that use activation to guide the distillation. Although attention provides inherent hints for discriminative areas, the relation between these regions and knowledgeable regions is still unclear. To further improve KD quality, we hope to provide an explicit solution to connect the desired knowledge with feature selection.

Towards this goal, we present **I**nstance-**C**onditional knowledge **D**istillation (ICD), which introduces a new KD framework based-on conditional Knowledge retrieval. In ICD, we propose a decoding network to find and distill knowledge that contributed to different instances, we deem such knowledge as instance-conditional knowledge. Fig. 1 shows the framework and compares it with former ones, ICD learns to find desired knowledge, other than using designed rules. In detail, we design a conditional decoding module to locate knowledge, the correlation between knowledge and each instance is computed by the instance-aware attention via the transformer decoder [5, 43]. In which each human observed instance is projected to query and the correlation is measured by scaled-product attention between query and teacher's representations. Next, we introduce an auxiliary task to optimize the decoding module, it teaches the decoder to find useful information for identification and localization, which is fundamental for detection. The task only facilitates the decoder, instead of the student. Lastly, we perform distillation over features decomposed by the decoder and weighted by the instance-aware attention. Our contribution is summarized in three-fold:

- We introduce a novel framework to locate useful knowledge in detection KD, we formulate the knowledge retrieval explicitly by a decoding network and optimize it via an auxiliary task.

- We adopt the conditional modeling paradigm to facilitate instance-wise knowledge transferring. We encode human observed instances as query and decompose teacher's representations to key and value to locate fine-grained knowledge. To our knowledge, it is the first trial to explore instance-oriented knowledge for detection.

- We perform comprehensive experiments on challenging benchmarks. Results demonstrate impressive improvements over various detectors with up to 4 AP gain in MS-COCO, including recent detectors for instance segmentation [41, 46, 16]. Under some cases, students with $1\times$ schedule are able to outperform their teachers with larger backbones trained $3\times$ longer.

2 Related Works

2.1 Knowledge Distillation

Knowledge distillation aims to transfer knowledge from a strong teacher to a weaker student network to facilitate supervised learning. The teacher is usually a large pretrained network, who provides smoother supervision and more hints on visual concepts, that improves the training quality and convergence speed [49, 9]. KD for image classification has been studied for years, they are usually categorized into three types [13]: response-based [19], feature-based [37, 43] and relation-based [32].

Among them, feature-based distillation over multi-scale features is adopted from most of detection KD works, to deal with knowledge among multiple instances in different regions. Most of these works can be formulated as region selection for distillation, where foreground-background unbalancing is considered as a key problem in some studies [45, 51, 14]. Under this paradigm, we divide them into three kinds: (1) prediction-based, (2) heuristics-based and (3) attention-based.

(1) Prediction-based methods rely on the prediction of the RPN or detection network to find foreground regions, *e.g.*, Chen *et al.* [6] and Li *et al.* [28] propose to distilling regions predicted by RPN [36], Dai *et al.* [11] proposes GI scores to locate controversial predictions for distillation.

(2) Heuristics-based methods rely on designed rules that can be inflexible and hyper-parameters inefficient, *e.g.*, Wang *et al.* [45] distill assigned regions where anchor and ground-truth have a large IoU, Guo *et al.* [14] distill foreground and background regions separately with different factors.

(3) Attention-based methods rely on activations to locate discriminative areas, yet they do not direct to knowledge that the student needs. Only a recent work from Zhang *et al.* [51] considers attention, they build the spatial-channel-wise attention to weigh the distillation.

To overcome the above limitations, we explore the instance-conditional knowledge retrieval formulated by a decoder to explicitly search for useful knowledge. Like other methods, ICD does not have extra cost during inference or use extra data (besides existing labels and a pretrained teacher).

2.2 Conditional Computation

Conditional computation is widely adopted to infer contents on a given condition. Our study mostly focuses on how to identify visual contents given an instance as a condition. This is usually formulated as query an instance on the image, *e.g.*, visual question answer [1, 2] and image-text matching [26] queries information and regions specified by natural language. Besides query by language, other types of query are proposed in recent years. For example, DETR [5] queries on fixed proposal embeddings, Chen *et al.* [8] encodes points as queries to facilitate weakly-supervised learning. These works adopt transformer decoder to infer upon global receptive fields that cover all visual contents, yet they usually rely on cascaded decoders that are costly for training. From another perspective, CondInst [41] and SOLOv2 [46] generate queries based on network predictions and achieves great performance on instance segmentation. Different from them, this work adopts the query-based approach to retrieve knowledge and build query based on annotated instances.

2.3 Object Detection

Object detection has been developed rapidly. Modern detectors are roughly divided into two-stage or one-stage detectors. Two-stage detectors usually adopt Region Proposal Network (RPN) to generate initial rough predictions and refine them with detection heads, the typical example is Faster R-CNN [36]. On the contrary, one-stage detectors directly predict on the feature map, which are usually faster, they include RetinaNet [30], FCOS [42]. Besides of this rough division, many extensions are introduced in recent years, *e.g.*, extension to instance segmentation [41, 46, 16], anchor-free models [42, 25] and end-to-end detection [5, 44, 20]. Among these works, multi-scale features are usually adopted to enhance performance, *e.g.*, FPN [29]. To generalize to various methods, the proposed method distills the intermediate features and does not rely on detector-specific designs.

3 Method

3.1 Overview

As discussed in former studies [14, 51], useful knowledge for detection distributes unevenly in intermediate features. To facilitate KD, we propose to transfer instance-conditional knowledge between student and teacher network, termed $\kappa_i^{\mathcal{S}}$ and $\kappa_i^{\mathcal{T}}$ corresponding to the i_{th} instance:

$$\mathcal{L}_{distill} = \sum_{i=1}^{N} \mathcal{L}_d(\kappa_i^{\mathcal{S}}, \kappa_i^{\mathcal{T}}) \tag{1}$$

The knowledge towards teacher representation $\mathcal{T}$ and condition y_i is formulated as $\kappa_i^{\mathcal{T}} = \mathcal{G}(\mathcal{T}, y_i)$ ($\kappa_i^{\mathcal{S}}$ similarly), where $\mathcal{G}$ is the instance-conditional decoding module, optimized by an auxiliary loss illustrated in Sec. 3.3. The overall framework is shown in Fig. 2.

In the following sections, we will introduce the instance-conditional knowledge (Sec. 3.2), describe the auxiliary task design (Sec. 3.3), and discuss the knowledge transferring (Sec. 3.4).

3.2 Instance-conditional Knowledge

In this section, we elaborate the instance-conditional decoding module $\mathcal{G}$, which computes instance-conditional knowledge $\kappa_i^{\mathcal{T}}$ from (1) *unconditional knowledge* given (2) *instance conditions*.

(1) The unconditional knowledge $\mathcal{T}$, symbolizes all available information from the teacher detector. Since modern detectors commonly involve a feature pyramid network (FPN) [29] to extract rich multi-scale representations, we present multi-scale representations as $\mathcal{T} = \{X_p \in \mathbb{R}^{D \times H_p \times W_p}\}_{p \in \mathcal{P}}$, where $\mathcal{P}$ signifies the spatial resolutions while D is the channel dimension. By concatenating representations at different scales along the spatial dimension, we obtain $\mathrm{A}^{\mathcal{T}} \in \mathbb{R}^{L \times D}$, where $L = \sum_{p \in \mathcal{P}} H_p W_p$ is the sum of total pixels number across scales.

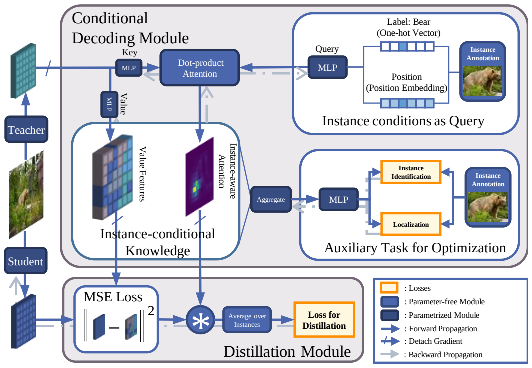

Figure 2: We propose a decoding module to retrieve knowledge via query-based attention, where instance annotations are encoded as a query. An auxiliary task is proposed to optimize the decoding module and the feature-based distillation loss weighted by the attention is used to update student.

(2) The instance condition, originally describing a human-observed object, is denoted by $\mathcal{Y} = \{\mathrm{y}_i\}_{i=1}^N$, where N is the object number and $\mathrm{y}_i = (c_i, \mathbf{b}_i)$ is the annotation for the i-th instance, including category c_i and box location $\mathbf{b}_i = (x_i, y_i, w_i, h_i)$ which specifies the localization and size information.

To produce learnable embeddings for each instance, the annotation is mapped to a *query* feature vector $\mathbf{q}_i$ in the hidden space, which specifies a condition to collect desired knowledge:

$$\mathbf{q}_i = \mathcal{F}_q(\mathcal{E}(\mathrm{y}_i)), \;\; \mathbf{q}_i \in \mathbb{R}^D \tag{2}$$

where $\mathcal{E}(\cdot)$ is a instance encoding function (detailed in in Sec. 3) and $\mathcal{F}_q$ is a Multi-Layer Perception network (MLP).

We retrieve knowledge from $\mathcal{T}$ given $\mathbf{q}_i$ by measuring responses of correlation. This is formulated by dot-product attention [43] with M concurrent heads in a query-key attention manner. In which each head j corresponds to three linear layers ($\mathcal{F}_j^k$, $\mathcal{F}_j^q$, $\mathcal{F}_j^v$) *w.r.t.* the key, query and value construction.

The key feature $\mathrm{K}_j^{\mathcal{T}}$ is computed by projecting teacher's representations $\mathrm{A}^{\mathcal{T}}$ with the positional embeddings [43, 5] $\mathrm{P} \in \mathbb{R}^{L \times d}$ as in Eq. 3, where $\mathcal{F}_{pe}$ denotes a linear projection over position embeddings. The value feature $\mathrm{V}_j^{\mathcal{T}}$ and query $\mathbf{q}_{ij}$ is projected by linear mappings to a sub-space with $d = D/M$ channels, $\mathcal{F}_j^v$ on $\mathrm{A}^{\mathcal{T}}$ and $\mathcal{F}_j^q$ over $\mathbf{q}_i$ respectively, as shown in Eq. 4. At last, an

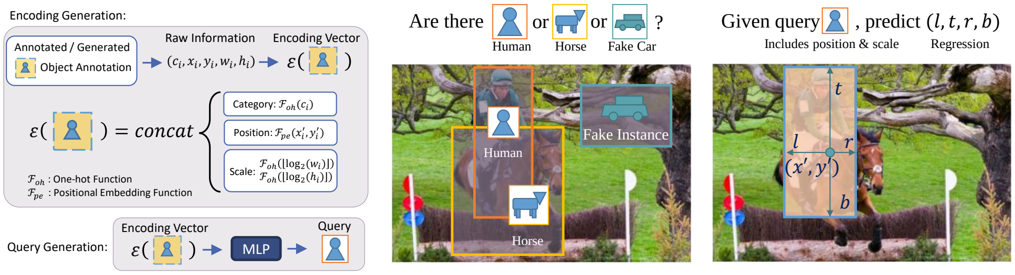
Encoding Generation:
Annotated / Generated
Object Annotation
Raw Information
Encoding Vector
$(c_i, x_i, y_i, w_i, h_i)$
$\mathcal{E}($ $)$
$\mathcal{E}($ $) = concat$
Category: $\mathcal{F}_{oh}(c_i)$
Position: $\mathcal{F}_{pe}(x'_i, y'_i)$
Scale: $\mathcal{F}_{oh}(\lfloor\log_2(w_i)\rfloor)$ $\mathcal{F}_{oh}(\lfloor\log_2(h_i)\rfloor)$
$\mathcal{F}_{oh}$: One-hot Function
$\mathcal{F}_{pe}$: Positional Embedding Function
Query Generation:
Encoding Vector
MLP
Query
Are there or or ?
Human
Horse
Fake Car
Fake Instance
Given query , predict (l, t, r, b)
Includes position & scale
Regression
t
l
r
(x', y')
b

(a) Encoding for instance conditions.

(b) Identification task.

(c) Localization task.

Figure 3: The illustration of the auxiliary task. (a) The instance encoding function encodes a instance condition to a vector, it is then projected as query features. (b) The identification task learns to identify the existence the queried instance. (c) The localization task learns to predict the boundary given an uncertain position provided by the query.

instance-aware attention mask $\mathbf{m}_{ij}$ of the i-th instance by the j-th head is obtained by normalized dot-product between $\mathrm{K}_j^{\mathcal{T}}$ and $\mathbf{q}_{ij}$:

$$\mathrm{K}_j^{\mathcal{T}} = \mathcal{F}_j^k(\mathrm{A}^{\mathcal{T}} + \mathcal{F}_{pe}(\mathrm{P})), \;\; \mathrm{K}_j^{\mathcal{T}} \in \mathbb{R}^{L \times d} \tag{3}$$

$$\mathrm{V}_j^{\mathcal{T}} = \mathcal{F}_j^v(\mathrm{A}^{\mathcal{T}}), \;\; \mathrm{V}_j^{\mathcal{T}} \in \mathbb{R}^{L \times d} \tag{4}$$

$$\mathbf{q}_{ij} = \mathcal{F}_j^q(\mathbf{q}_i), \;\; \mathbf{q}_{ij} \in \mathbb{R}^d \tag{5}$$

$$\mathbf{m}_{ij} = softmax(\frac{\mathrm{K}_j^{\mathcal{T}} \mathbf{q}_{ij}}{\sqrt{d}}), \;\; \mathbf{m}_{ij} \in \mathbb{R}^L \tag{6}$$

Intuitively, the querying along the key features and value features describes the correlation between representations and instances. We collect $\kappa_i^{\mathcal{T}} = \{(\mathbf{m}_{ij}, \mathrm{V}_j^{\mathcal{T}})\}_{j=1}^M$ as the instance-conditional knowledge from $\mathcal{T}$, which encodes knowledge corresponds to the ith instance.

3.3 Auxiliary Task

In this section, we introduce the auxiliary task to optimize the decoding module $\mathcal{G}$. First, we aggregate instance-level information to identify and localize objects. This could be obtained by aggregating the instance-conditional knowledge by the function $\mathcal{F}_{agg}$, which includes sum-product aggregation over attention $\mathbf{m}_{ij}$ and $\mathrm{V}_j^{\mathcal{T}}$, concatenate features from each head, add residuals and project with a feed-forward network as proposed in [43, 5]:

$$\mathbf{g}_i^{\mathcal{T}} = \mathcal{F}_{agg}(\kappa_i^{\mathcal{T}}, \mathbf{q}_i), \;\; \mathbf{g}_i^{\mathcal{T}} \in \mathbb{R}^D \tag{7}$$

To let the instance-level aggregated information $\mathbf{g}_i^{\mathcal{T}}$ retain sufficient instance cues, one could design an instance-sensitive task to optimize it as below:

$$\mathcal{L}_{aux} = \mathcal{L}_{ins}(\mathbf{g}_i^{\mathcal{T}}, \mathcal{H}(\mathrm{y}_i)) \tag{8}$$

where $\mathcal{H}$ encodes the instance information as targets. However, directly adopt Eq. 8 might lead to trivial solution, since y_i is accessible from both $\mathbf{g}_i^{\mathcal{T}}$ (through $\mathbf{q}_i$, see Eq. 2) and $\mathcal{H}(\mathrm{y}_i)$. It is possible that parameters will learn a shortcut, that ignore the teacher representations $\mathcal{T}$. To resolve this issue, we propose to drop information on encoding function $\mathcal{E}(\cdot)$, to force the aggregation function $\mathcal{F}_{agg}$ to excavate hints from $\mathcal{T}$.

The information dropping is adopted by replacing the accurate annotation for instance conditions to uncertain ones. For bounding box annotations, we relieve them to rough box centers with rough scales indicators. The rough box center (x'_i, y'_i) is obtained by random jittering as shown below:

$$\begin{cases} x'_i = x_i + \phi_x w_i, \\ y'_i = y_i + \phi_y h_i, \end{cases} \tag{9}$$

where (w_i, h_i) is the width and height of the bounding box and ϕ_x, ϕ_y are sampled from a uniform distribution $\Phi \sim U[-a, a]$, where we set a=0.3 empirically. The scales indicators are obtained by rounding the box sizes in the logarithmic space, *i.e.*, $\lfloor log_2(w_i) \rfloor$, $\lfloor log_2(h_i) \rfloor$. In addition, to let the decoder learn to identify instances and be aware of the uncertainty, we generate fake instances for the identification task according to dataset distributions, this is detailed in Appendix A. As a result, it collect coarse information and obtain instance encoding through $\mathcal{E}(\cdot)$ as depicted in Fig. 3a. where c_i is the category, $\mathcal{F}_{oh}$ is the one hot vectorization, $concat$ is the concatenation operator and $\mathcal{F}_{pe}$ is the position embedding function.

Finally, the aggregated representation $\mathbf{g}_i^{\mathcal{T}}$ are optimized by the auxiliary task. We introduces two predictors denoted by $\mathcal{F}_{obj}$ and $\mathcal{F}_{reg}$ respectively to predict identification and localization results. We adopt binary cross entropy loss (BCE) to optimize the real-fake identification and $L1$ loss to optimize the regression.

$$\mathcal{L}_{aux} = \mathcal{L}_{BCE}(\mathcal{F}_{obj}(\mathbf{g}_i^{\mathcal{T}}), \delta_{obj}(\mathrm{y}_i)) + \mathcal{L}_1(\mathcal{F}_{reg}(\mathbf{g}_i^{\mathcal{T}}), \delta_{reg}(\mathrm{y}_i)) \tag{10}$$

where $\delta_{obj}(\cdot)$ is an indicator, it yields 1 if y_i is real and 0 otherwise. Following common practice, the localization loss for fake examples is ignored. δ_{reg} is the preparing function for regression targets, following [42]. Appendix A provides more implementation details.

3.4 Instance-Conditional Distillation

Lastly, we present the formulation for conditional knowledge distillation. We obtain the projected value features $\mathrm{V}_j^{\mathcal{S}} \in \mathbb{R}^{L \times d}$ of the student representations analogous to Eq. 4 in Sec. 3.2. By adopting the instance-aware attention mask as a measurement of correlations between feature and each instance, we formulate the distillation loss as value features mimicking guided by the attention:

$$\mathcal{L}_{distill} = \frac{1}{MN_r} \sum_{j=1}^{M} \sum_{i=1}^{N} \delta_{obj}(\mathrm{y}_i) \cdot < \mathbf{m}_{ij}, \mathcal{L}_{MSE}(\mathrm{V}_j^{\mathcal{S}}, \mathrm{V}_j^{\mathcal{T}}) > \tag{11}$$

where $N_r = \sum_{i=1}^{N} \delta_{obj}(\mathrm{y}_i)$, $(N_r \leq N)$ is the real instances number, $\mathcal{L}_{MSE}(\mathrm{V}_j^{\mathcal{S}}, \mathrm{V}_j^{\mathcal{T}}) \in \mathbb{R}^L$ is the pixel-wise mean-square error along the hidden dimension[2] and $< \cdot, \cdot >$ is the Dirac notation for inner product. For stability, the learnable variable $\mathbf{m}_{ij}$ and $\mathrm{V}_j^{\mathcal{T}}$ are detached during distillation. Combine with the supervised learning loss $\mathcal{L}_{det}$, the overall loss with a coefficient λ is summarized below:

$$\mathcal{L}_{total} = \mathcal{L}_{det} + \mathcal{L}_{aux} + \lambda \mathcal{L}_{distill} \tag{12}$$

It is worth noticing, only the gradients *w.r.t.* $\mathcal{L}_{distill}$ and $\mathcal{L}_{det}$ back-propagate to the student network (from representations $\mathcal{S}$). The gradients of $\mathcal{L}_{aux}$ only update the instance-conditional decoding function $\mathcal{G}$ and auxiliary task related modules.

4 Experiments

4.1 Experiment Settings

We conduct experiments on Pytorch [34] with the widely used Detectron2 library [47] and AdelaiDet library [3] [40]. All experiments are running on eight 2080ti GPUs with 2 images in each. We adopt the $1\times$ scheduler, which denotes 9k iterations of training, following the standard protocols in Detectron2 unless otherwise specified. Scale jittering with random flip is adopted as data augmentation.

For distillation, the hyper-parameter λ is set to 8 for one-stage detectors and 3 for two-stage detectors respectively. To optimize the transformer decoder, we adopt AdamW optimizer [33] for the decoder and MLPs following common settings for transformer [43, 5]. Corresponding hyper-parameters follows [5], where the initial learning rate and weight decay are set to 1e-4. We adopt the 256 hidden dimension for our decoder and all MLPs, the decoder has 8 heads in parallel. The projection layer $\mathcal{F}_q$ is a 3 layer MLP, F_{reg} and F_{obj} share another 3 layer MLP. In addition, we notice some newly initialized modules of the student share the same size of the teacher, *e.g.*, the detection head, FPN.

[2] $\mathcal{L}_{MSE}(.)$ is conducted over normalized features with parameter-free LayerNorm [3] for stabilization.

[3] All libraries are open-sourced and public available, please refer to citations for more details.

Table 1: Comparison with previous methods on challenging benchmark MS-COCO. The method proposed by Li *et al.* [28] does not apply to RetinaNet. † denotes the inheriting strategy.

Method	Faster R-CNN [36]				RetinaNet [30]			
	AP	AP_S	AP_M	AP_L	AP	AP_S	AP_M	AP_L
Teacher w. ResNet-101 (3×)	42.0	25.2	45.6	54.6	40.4	24.0	44.3	52.2
Student w. ResNet-50 (1×)	37.9	22.4	41.1	49.1	37.4	23.1	41.6	48.3
+ FitNet [37]	39.3 (+1.4)	22.7	42.3	51.7	38.2 (+0.8)	21.8	42.6	48.8
+ Li *et al.* [28]	39.5 (+1.5)	23.3	43.0	51.4	-	-	-	-
+ Wang *et al.* [45]	39.2 (+1.3)	23.2	42.8	50.4	38.4 (+1.0)	23.3	42.6	49.1
+ Zhang *et al.* [51]	40.0 (+2.1)	23.2	43.3	52.5	39.3 (+1.9)	23.4	43.6	50.6
+ Ours	40.4 (+2.5)	23.4	44.0	52.0	39.9 (+2.5)	25.0	43.9	51.0
+ Ours †	40.9 (+3.0)	24.5	44.2	53.5	40.7 (+3.3)	24.2	45.0	52.7

Table 2: Experiments on more detectors with ICD. Type denotes the AP score is evaluated on bounding box (`BBox`) or instance mask (`Mask`). † denotes using the inheriting strategy.

Detector	Setting	Type	AP	AP_{50}	AP_{75}	AP_S	AP_M	AP_L
FCOS [42] Teacher: 18.8 FPS / 51.2M Student: 25.0 FPS / 32.2M	Teacher (3×)	`BBox`	42.6	61.6	45.8	26.2	46.3	53.8
	Student (1×)		39.4	58.2	42.4	24.2	43.4	49.4
	+ Ours		41.7(+2.3)	60.3	45.4	26.9	45.9	52.6
	+ Ours †		42.9(+3.5)	61.6	46.6	27.8	46.8	54.6
Mask R-CNN [16] Teacher: 17.5 FPS / 63.3M Student: 22.9 FPS / 44.3M	Teacher (3×)	`BBox`	42.9	63.3	46.8	26.4	46.6	56.1
	Student (1×)		38.6	59.5	42.1	22.5	42.0	49.9
	+ Ours		40.4 (+1.8)	60.9	44.2	24.4	43.7	52.0
	+ Ours †		41.2 (+2.6)	62.0	45.0	25.1	44.5	53.6
	Teacher (3×)	`Mask`	38.6	60.4	41.3	19.5	41.3	55.3
	Student (1×)		35.2	56.3	37.5	17.2	37.7	50.3
	+ Ours		36.7 (+1.5)	58.0	39.2	18.4	38.9	52.5
	+ Ours †		37.4 (+2.2)	58.7	40.1	19.1	39.8	53.7
SOLOv2 [46] Teacher: 16.6 FPS / 65.5M Student: 21.4 FPS / 46.5M	Teacher (3×)	`Mask`	39.0	59.4	41.9	16.2	43.1	58.2
	Student		34.6	54.7	36.9	13.2	37.9	53.3
	+ Ours		37.2 (+2.6)	57.6	39.8	14.8	40.7	57.0
	+ Ours †		38.5 (+3.9)	59.0	41.2	15.9	42.3	58.9
CondInst [41] Teacher: 16.8 FPS / 53.5M Student: 21.3 FPS / 34.1M	Teacher (3×)	`BBox`	44.6	63.7	48.4	27.5	47.8	58.4
	Student (1×)		39.7	58.8	43.1	23.9	43.3	50.1
	+ Ours		42.4 (+2.7)	61.5	46.1	25.3	46.0	54.3
	+ Ours †		43.7 (+4.0)	62.9	47.2	27.1	47.3	56.6
	Teacher (3×)	`Mask`	39.8	61.4	42.6	19.4	43.5	58.3
	Student (1×)		35.7	56.7	37.7	16.8	39.1	50.3
	+ Ours		37.8 (+2.1)	59.1	40.4	17.5	41.4	54.7
	+ Ours †		39.1 (+3.4)	60.5	42.0	19.1	42.6	57.0

We find initialize these modules with teacher's parameters will lead to faster convergence, we call it the inheriting strategy in experiments.

Most experiments are conducted on a large scale object detection benchmark **MS-COCO** [4][31] with 80 classes. We train models on MS-COCO 2017 `trainval115k` subset and validate on `minival` subset. Following common protocols, we report mean Average Precision (AP) as an evaluation metric, together with AP under different thresholds and scales, *i.e.*, AP_{50}, AP_{75}, AP_S, AP_M, AP_L. Other experiments are listed in Appendix B, e.g., on VOC [12] and Cityscapes [10], more ablations.

4.2 Main Results

Compare with state-of-the-art methods. We compare our method (ICD) with previous state-of-the-arts (SOTAs), including a classic distillation method FitNet [37], two typical detection KD methods [28, 45], and a very recent work with strong performance from Zhang *et al.* [51]. The comparison is conducted on two classic detectors: Faster R-CNN [36] and RetinaNet [30]. We adopt

[4] MS-COCO is publicly available, the annotations are licensed under a `Creative Commons Attribution 4.0 License` and the use of the images follows `Flickr Terms of Use`. Refer to [31] for more details.

Table 3: Experiments on mobile backbones. † denotes using the inheriting strategy.

Detector	Setting	Backbone	AP	AP$_{50}$	AP$_{75}$	AP$_{\mathrm{S}}$	AP$_{\mathrm{M}}$	AP$_{\mathrm{L}}$
RetinaNet [30]	Teacher (3×)	ResNet-101 [17]	40.4	60.3	43.2	24.0	44.3	52.2
	Student (1×)	MBV2 [38]	26.4	42.0	27.8	13.8	28.8	34.1
	+ Ours		29.5 (+3.1)	45.5	31.2	16.2	32.2	38.3
	+ Ours †		31.6 (+5.2)	48.5	33.4	17.6	34.7	41.3
RetinaNet [30]	Teacher (3×)	ResNet-101 [17]	40.4	60.3	43.2	24.0	44.3	52.2
	Student (1×)	Eff-B0 [39]	34.9	54.8	37.0	20.9	38.9	44.8
	+ Ours		36.7 (+1.8)	56.0	38.7	21.1	40.6	48.1
	+ Ours †		38.0 (+3.1)	57.5	40.2	22.4	41.6	50.3
FRCNN [36]	Teacher (3×)	ResNet-101 [17]	42.0	62.5	45.9	25.2	45.6	54.6
	Student (1×)	MBV2 [38]	27.2	44.7	28.8	14.6	29.6	35.6
	+ Ours		30.2 (+3.0)	48.0	32.5	17.0	32.2	39.1
	+ Ours †		31.4 (+4.2)	49.4	33.6	17.6	33.5	41.3
FRCNN [36]	Teacher (3×)	ResNet-101 [17]	42.0	62.5	45.9	25.2	45.6	54.6
	Student (1×)	Eff-B0 [39]	35.3	56.8	37.8	20.8	38.2	45.1
	+ Ours		37.0 (+1.7)	58.0	39.6	21.1	40.0	48.3
	+ Ours †		37.9 (+2.6)	58.7	40.8	21.4	40.9	49.5

detectron2 official released models with ResNet-101 backbone trained on 3× scheduler as teacher networks, the student is trained on 1× with ResNet-50 backbone following the above settings.

As shown in Table 1, ICD brings about 2.5 AP and 3.0 AP improvement for plain training and training with the inheriting strategy respectively. Especially for RetinaNet, the student with distillation even outperforms a strong teacher trained on 3× scheduler. Compare with previous SOTAs, the proposed method leads to a considerable margin for about 0.5 AP without the inheriting strategy.

Results on other settings. We further evaluate ICD under various detectors, *e.g.*, a commonly used anchor-free detector FCOS [42], and three detectors that have been extended to instance segmentation: Mask R-CNN [16], SOLOv2 [46] and CondInst [41]. We adopt networks with ResNet-101 on 3× scheduler as teachers and networks with ResNet-50 on 1× scheduler as students following the above settings. As shown in Table 2, we observe consistent improvements for both detection and instance segmentation. There are at most around 4 AP improvement on CondInst [41] on object detection and SOLOv2 [46] on instance segmentation. Moreover, students with weaker backbone (ResNet-50 *v.s.* ResNet-101) and less training images (1/3) even outperform (FCOS) or perform on par (SOLOv2, CondInst) with teachers. Note that ICD does not introduce extra burden during inference, our method improves about 25% of FPS[5] and reduces 40% of parameters compared with teachers.

Mobile backbones. Aside from main experiments on commonly used ResNet [17], we also conduct experiments on mobile backbones, which are frequently used in low-power devices. We evaluate our method on two prevalent architectures: MobileNet V2 (MBV2) [38] and EfficientNet-B0 (Eff-B0) [39]. The latter one adopts the MobileNet V2 as basis, and further extends it with advanced designs like stronger data augmentation and better activations.

Experiments are conducted on Faster R-CNN (*abbr.*, FRCNN) [36] and RetinaNet [30] following the above settings. As shown in Table 3, our method also significantly improves the performance on smaller backbones. For instance, we improve the RetinaNet with MobileNet V2 backbone with 5.2 AP gain and 3.1 AP gain with and without inheriting strategy respectively, and up to 3.1 AP gain for EfficientNet-B0. We also observe consistent improvements over Faster R-CNN, with up to 4.2 AP gain for MobileNet-V2 and 2.6 AP gain for EfficientNet-B0.

4.3 Ablation Studies

To verify the design options and the effectiveness of each component, we conduct ablation studies with the classic RetinaNet detector on MS-COCO following the above settings.

Design of the auxiliary task. To better understand the role of our auxiliary task, we conduct experiments to evaluate the contribution of each sub-task. Specifically, our auxiliary task is composed

[5] FPS is evaluated on Nvidia Tesla V100.

of an identification task with binary cross-entropy loss and a localization task with regression loss, the localization task is further augmented with a hint on bounding box scales. As shown in Table 4, the identification task itself leads to 2.2 AP gain compare with the baseline, this high-light the importance of knowledge on object perception. The regression task itself leads to 1.8 AP gain, and the scale information boosts it for extra 0.2 AP gain. Combine two of them, we achieve 2.5 AP overall improvement, which indicates the fusion of two knowledge brings extra benefits. Note the auxiliary task only update the decoder and does not introduce extra data, which is very different from multitask learning, *e.g.*, Mask R-CNN[16].

Table 4: Comparison with different auxiliary task designs.

Identification	Localization	+ Scale	AP	AP_{50}	AP_{75}	AP_{S}	AP_{M}	AP_{L}
			37.4	56.7	40.3	23.1	41.6	48.3
✓			39.6	59.2	42.8	23.4	44.0	50.4
	✓		39.2	58.6	42.4	23.1	43.5	50.3
	✓	✓	39.4	58.8	42.4	23.2	43.8	50.5
✓	✓	✓	39.9	59.4	43.1	25.0	43.9	51.0

Impact of the instance-aware attention. To verify the effectiveness of instance-aware attention learned by conditional computation, we directly replace it with different variations: the fine-grained mask in [45], pixel-wise attention activation [51, 43], foreground mask analog to [14] and no attention mask. The result in Fig. 5 shows our instance-aware mask leads to about 0.9 AP gain over the baseline and 0.4 AP gain compare with the best replacement.

Table 5: Comparison with different types of attention.

Attention Type	AP	AP_{50}	AP_{75}	AP_{S}	AP_{M}	AP_{L}
No Attention	39.0	58.4	42.1	23.5	43.2	49.9
Foreground Mask	39.4	58.9	42.4	23.5	43.6	50.0
Fine-grained Mask [45]	39.5	59.0	42.4	23.4	43.8	50.2
Attention Activation [43]	39.3	58.6	42.3	22.6	43.6	50.1
Instance-conditional Attention	39.9	59.4	43.1	25.0	43.9	51.0

Design of the decoder. We mainly verify two properties of the decoder design, as shown in Table 6. First, we find a proper number of heads is important for the best performance. The head number balances the dimension for each sub-space and the number of spaces. The best number lies around 8, which is consistent with former studies [5]. Second, we evaluate the effectiveness of cascaded decoders, as it is widely adopted in former studies [43, 5, 8]. However, we do not find significant differences between different cascade levels, it might because we use a fixed teacher to provide knowledge, that limited the learning ability.

Table 6: Ablation on the number of heads and cascade levels.

(a) Number of heads.

Heads	AP	AP_{S}	AP_{M}	AP_{L}
1	39.4	23.7	43.8	50.5
4	39.7	24.0	43.9	51.2
8	39.9	25.0	43.9	51.0
16	39.7	23.6	44.2	50.5

(b) Number of cascade levels.

Levels	AP	AP_{S}	AP_{M}	AP_{L}
1	39.9	25.0	43.9	51.0
2	39.9	24.1	44.0	51.4
4	39.8	24.3	44.0	50.9

5 Discussion

Qualitative analysis. We present a visualization of our learned instance-aware attention in Fig. 4. We find different heads attend to different components related to each instance, *e.g.*, salient parts, boundaries. This might suggest that salient parts are important and knowledge for regression mostly lies around boundaries, instead of averaged on the foreground as assumed in former studies. The head (vi) and (vii) are smoother around key regions, which may relate to context. The head (iv) mainly attends on image corners, which might be a degenerated case or relate to some implicit descriptors.

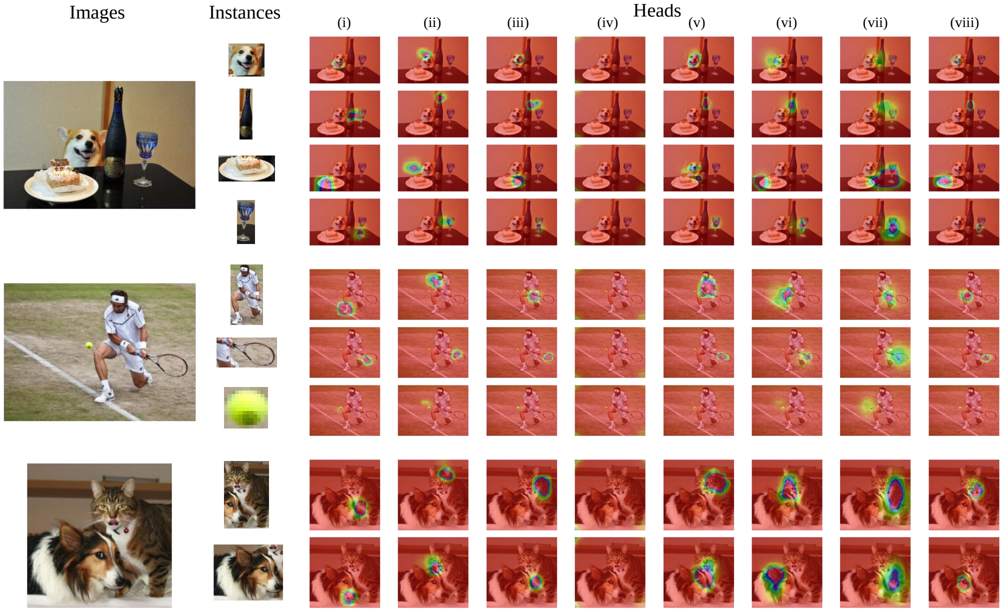

Figure 4: Visualization of our learned instance-aware attention over each head. Red denotes weak areas and pink denotes strong areas.

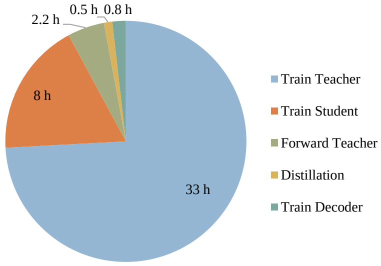

Figure 5: Time consumption.

Resource consumption. We benchmark the training speed for our distillation method. As shown in Fig. 5, training the decoder introduces negligible cost. Specifically, we benchmark on 1× scheduler on RetinaNet [30] with eight 2080ti, following the same configuration in Section 4.2. The major time consumption is spent on training the teacher (3×), which takes about 33 hours. Training (forward and backward) the student takes about 8 hours, while training decoder and distillation only take 1.3 hours. Besides the training time, memory consumption of our method is also limited. One can update the decoder part and the student part in consecutive iterations, leaving only intermediate features for distillation in memory across iterations.

Real-world impact. The proposed method provides a convenient approach to enhance a detector under a certain setting, resulting in that a small model can perform on par with a larger one. On the positive side, it allows users to replace a big model with a smaller one, which reduces energy consumption. On the potentially negative side, the teacher could be costly in training, also the student might inherit biases from the teacher, which is hard for tracing.

6 Conclusion

We propose a novel framework for knowledge distillation. The proposed **I**nstance-**C**onditional knowledge **D**istillation (ICD) method utilizes instance-feature cross attention to select and locate knowledge that correlates with human observed instances, which provides a new framework for KD. Our formulation encodes instance as query and teacher's representation as key. To teach the decoder how to find knowledge, we design an auxiliary task that relies on knowledge for recognition and localization. The proposed method consistently improves various detectors, leading to impressive performance gain, some student networks even surpass their teachers. In addition to our design of the auxiliary task, we believe there are other alternations that can cover different situations or provide a theoretical formulation of knowledge, which will be a potential direction for further researches.

Acknowledgments and Disclosure of Funding

This paper is supported by the National Key R&D Plan of the Ministry of Science and Technology (Project No. 2020AAA0104400) and Beijing Academy of Artificial Intelligence (BAAI).

References

[1] Peter Anderson, Xiaodong He, Chris Buehler, Damien Teney, Mark Johnson, Stephen Gould, and Lei Zhang. Bottom-up and top-down attention for image captioning and visual question answering. In *CVPR*, 2018.

[2] Stanislaw Antol, Aishwarya Agrawal, Jiasen Lu, Margaret Mitchell, Dhruv Batra, C. Lawrence Zitnick, and Devi Parikh. VQA: visual question answering. In *ICCV*, 2015.

[3] Jimmy Lei Ba, Jamie Ryan Kiros, and Geoffrey E Hinton. Layer normalization. *ArXiv preprint*, 2016.

[4] Zhaowei Cai and Nuno Vasconcelos. Cascade r-cnn: Delving into high quality object detection. In *CVPR*, 2018.

[5] Nicolas Carion, Francisco Massa, Gabriel Synnaeve, Nicolas Usunier, Alexander Kirillov, and Sergey Zagoruyko. End-to-end object detection with transformers. In *ECCV*, 2020.

[6] Guobin Chen, Wongun Choi, Xiang Yu, Tony X. Han, and Manmohan Chandraker. Learning efficient object detection models with knowledge distillation. In *NeurIPS*, 2017.

[7] Kai Chen, Jiaqi Wang, Jiangmiao Pang, Yuhang Cao, Yu Xiong, Xiaoxiao Li, Shuyang Sun, Wansen Feng, Ziwei Liu, Jiarui Xu, Zheng Zhang, Dazhi Cheng, Chenchen Zhu, Tianheng Cheng, Qijie Zhao, Buyu Li, Xin Lu, Rui Zhu, Yue Wu, Jifeng Dai, Jingdong Wang, Jianping Shi, Wanli Ouyang, Chen Change Loy, and Dahua Lin. MMDetection: Open mmlab detection toolbox and benchmark. *arXiv preprint arXiv:1906.07155*, 2019.

[8] Liangyu Chen, Tong Yang, Xiangyu Zhang, Wei Zhang, and Jian Sun. Points as queries: Weakly semi-supervised object detection by points. In *CVPR*, 2021.

[9] Xu Cheng, Zhefan Rao, Yilan Chen, and Quanshi Zhang. Explaining knowledge distillation by quantifying the knowledge. In *CVPR*, 2020.

[10] Marius Cordts, Mohamed Omran, Sebastian Ramos, Timo Rehfeld, Markus Enzweiler, Rodrigo Benenson, Uwe Franke, Stefan Roth, and Bernt Schiele. The cityscapes dataset for semantic urban scene understanding. In *CVPR*, 2016.

[11] Xing Dai, Zeren Jiang, Zhao Wu, Yiping Bao, Zhicheng Wang, Si Liu, and Erjin Zhou. General instance distillation for object detection. In *CVPR*, 2021.

[12] M. Everingham, S. M. A. Eslami, L. Van Gool, C. K. I. Williams, J. Winn, and A. Zisserman. The pascal visual object classes challenge: A retrospective. *IJCV*, 2015.

[13] Jianping Gou, Baosheng Yu, Stephen J Maybank, and Dacheng Tao. Knowledge distillation: A survey. *IJCV*, 2021.

[14] Jianyuan Guo, Kai Han, Yunhe Wang, Han Wu, Xinghao Chen, Chunjing Xu, and Chang Xu. Distilling object detectors via decoupled features. In *CVPR*, 2021.

[15] Song Han, Jeff Pool, John Tran, and William J Dally. Learning both weights and connections for efficient neural networks. In *NeurIPS*, 2015.

[16] Kaiming He, Georgia Gkioxari, Piotr Dollár, and Ross B. Girshick. Mask R-CNN. In *ICCV*, 2017.

[17] Kaiming He, Xiangyu Zhang, Shaoqing Ren, and Jian Sun. Deep residual learning for image recognition. In *CVPR*, 2016.

[18] Yihui He, Xiangyu Zhang, and Jian Sun. Channel pruning for accelerating very deep neural networks. In *ICCV*, 2017.

[19] Geoffrey Hinton, Oriol Vinyals, and Jeff Dean. Distilling the knowledge in a neural network. In *NeurIPS*, 2014.

[20] Han Hu, Jiayuan Gu, Zheng Zhang, Jifeng Dai, and Yichen Wei. Relation networks for object detection. In *CVPR*, 2018.

[21] Gao Huang, Zhuang Liu, Laurens van der Maaten, and Kilian Q. Weinberger. Densely connected convolutional networks. In *CVPR*, 2017.

[22] Itay Hubara, Matthieu Courbariaux, Daniel Soudry, Ran El-Yaniv, and Yoshua Bengio. Binarized neural networks. In *NeurIPS*, 2016.

[23] Itay Hubara, Matthieu Courbariaux, Daniel Soudry, Ran El-Yaniv, and Yoshua Bengio. Quantized neural networks: Training neural networks with low precision weights and activations. *JMLR*, 2017.

[24] Alex Krizhevsky, Ilya Sutskever, and Geoffrey E. Hinton. Imagenet classification with deep convolutional neural networks. In *NeurIPS*, 2012.

[25] Hei Law and Jia Deng. Cornernet: Detecting objects as paired keypoints. In *ECCV*, 2018.

[26] Kuang-Huei Lee, Xi Chen, Gang Hua, Houdong Hu, and Xiaodong He. Stacked cross attention for image-text matching. In *ECCV*, 2018.

[27] Hao Li, Asim Kadav, Igor Durdanovic, Hanan Samet, and Hans Peter Graf. Pruning filters for efficient convnets. In *ICLR*, 2017.

[28] Quanquan Li, Shengying Jin, and Junjie Yan. Mimicking very efficient network for object detection. In *CVPR*, 2017.

[29] Tsung-Yi Lin, Piotr Dollár, Ross B. Girshick, Kaiming He, Bharath Hariharan, and Serge J. Belongie. Feature pyramid networks for object detection. In *CVPR*, 2017.

[30] Tsung-Yi Lin, Priya Goyal, Ross B. Girshick, Kaiming He, and Piotr Dollár. Focal loss for dense object detection. In *ICCV*, 2017.

[31] Tsung-Yi Lin, Michael Maire, Serge Belongie, James Hays, Pietro Perona, Deva Ramanan, Piotr Dollár, and C Lawrence Zitnick. Microsoft coco: Common objects in context. In *ECCV*, 2014.

[32] Yufan Liu, Jiajiong Cao, Bing Li, Chunfeng Yuan, Weiming Hu, Yangxi Li, and Yunqiang Duan. Knowledge distillation via instance relationship graph. In *CVPR*, 2019.

[33] Ilya Loshchilov and Frank Hutter. Decoupled weight decay regularization. In *ICLR*, 2019.

[34] Adam Paszke, Sam Gross, Francisco Massa, Adam Lerer, James Bradbury, Gregory Chanan, Trevor Killeen, Zeming Lin, Natalia Gimelshein, Luca Antiga, Alban Desmaison, Andreas Köpf, Edward Yang, Zachary DeVito, Martin Raison, Alykhan Tejani, Sasank Chilamkurthy, Benoit Steiner, Lu Fang, Junjie Bai, and Soumith Chintala. Pytorch: An imperative style, high-performance deep learning library. In *NeurIPS*, 2019.

[35] Mohammad Rastegari, Vicente Ordonez, Joseph Redmon, and Ali Farhadi. Xnor-net: Imagenet classification using binary convolutional neural networks. In *ECCV*, 2016.

[36] Shaoqing Ren, Kaiming He, Ross B. Girshick, and Jian Sun. Faster R-CNN: towards real-time object detection with region proposal networks. In *NeurIPS*, 2015.

[37] Adriana Romero, Nicolas Ballas, Samira Ebrahimi Kahou, Antoine Chassang, Carlo Gatta, and Yoshua Bengio. Fitnets: Hints for thin deep nets. In *ICLR*, 2015.

[38] Mark Sandler, Andrew G. Howard, Menglong Zhu, Andrey Zhmoginov, and Liang-Chieh Chen. Mobilenetv2: Inverted residuals and linear bottlenecks. In *CVPR*, 2018.

[39] Mingxing Tan and Quoc V. Le. Efficientnet: Rethinking model scaling for convolutional neural networks. In *ICML*, Proceedings of Machine Learning Research, 2019.

[40] Zhi Tian, Hao Chen, Xinlong Wang, Yuliang Liu, and Chunhua Shen. AdelaiDet: A toolbox for instance-level recognition tasks. `https://git.io/adelaidet`, 2019.

[41] Zhi Tian, Chunhua Shen, and Hao Chen. Conditional convolutions for instance segmentation. In *Proc. Eur. Conf. Computer Vision (ECCV)*, 2020.

[42] Zhi Tian, Chunhua Shen, Hao Chen, and Tong He. FCOS: fully convolutional one-stage object detection. In *ICCV*, 2019.

[43] Ashish Vaswani, Noam Shazeer, Niki Parmar, Jakob Uszkoreit, Llion Jones, Aidan N. Gomez, Lukasz Kaiser, and Illia Polosukhin. Attention is all you need. In *NeurIPS*, 2017.

[44] Jianfeng Wang, Lin Song, Zeming Li, Hongbin Sun, Jian Sun, and Nanning Zheng. End-to-end object detection with fully convolutional network. In *CVPR*, 2021.

[45] Tao Wang, Li Yuan, Xiaopeng Zhang, and Jiashi Feng. Distilling object detectors with fine-grained feature imitation. In *CVPR*, 2019.

[46] Xinlong Wang, Rufeng Zhang, Tao Kong, Lei Li, and Chunhua Shen. SOLOv2: Dynamic and fast instance segmentation. In *NeurIPS*, 2020.

[47] Yuxin Wu, Alexander Kirillov, Francisco Massa, Wan-Yen Lo, and Ross Girshick. Detectron2. `https://github.com/facebookresearch/detectron2`, 2019.

[48] Jianwei Yang, Jiasen Lu, Dhruv Batra, and Devi Parikh. A faster pytorch implementation of faster r-cnn. `https://github.com/jwyang/faster-rcnn.pytorch`, 2017.

[49] Li Yuan, Francis E. H. Tay, Guilin Li, Tao Wang, and Jiashi Feng. Revisiting knowledge distillation via label smoothing regularization. In *CVPR*, 2020.

[50] Sergey Zagoruyko and Nikos Komodakis. Paying more attention to attention: Improving the performance of convolutional neural networks via attention transfer. In *ICLR*, 2017.

[51] Linfeng Zhang and Kaisheng Ma. Improve object detection with feature-based knowledge distillation: Towards accurate and efficient detectors. In *ICLR*, 2021.